Universality of pseudogap and emergent order in lightly doped Mott insulators

I. Battisti[1]*, K.M. Bastiaans[1]*, V. Fedoseev[1], A. de la Torre[2,3], N. Iliopoulos[1], A. Tamai[2], E.C. Hunter[4], R.S. Perry[5], J. Zaanen[1], F. Baumberger[2,6], M.P. Allan[1¶]

[1] *Leiden Institute of Physics, Leiden University, Niels Bohrweg 2, 2333 CA Leiden, The Netherlands*
[2] *Department of Quantum Matter Physics, University of Geneva, 24 Quai Ernest-Ansermet, 1211 Geneva 4, Switzerland*
[3] *Department of Physics, California Institute of Technology, Pasadena, California 91125, USA*
[4] *School of Physics and Astronomy, The University of Edinburgh, James Clerk Maxwell Building, Mayfield Road, Edinburgh EH9 2TT, United Kingdom*
[5] *London Centre for Nanotechnology and UCL Centre for Materials Discovery, University College London, London WC1E 6BT, United Kingdom*
[6] *Swiss Light Source, Paul Scherrer Institute, CH-5232 Villigen PSI, Switzerland*
** these authors contributed equally to this work; ¶ allan@physics.leidenuniv.nl*

1 It is widely believed that high-temperature superconductivity in the cuprates emerges from doped Mott insulators[1]. The physics of the parent state seems deceivingly simple: The hopping of the electrons from site to site is prohibited because their on-site Coulomb repulsion *U* is larger than the kinetic energy gain *t*. When doping these materials by inserting a small percentage of extra carriers, the electrons become mobile but the strong correlations from the Mott state are thought to survive; inhomogeneous electronic order, a mysterious pseudogap and, eventually, superconductivity appear. How the insertion of dopant atoms drives this evolution is not known, nor whether these phenomena are mere distractions specific to hole-doped cuprates or represent the genuine physics of doped Mott insulators. Here, we visualize the evolution of the electronic states of $(Sr_{1-x}La_x)_2IrO_4$, which is an effective spin-½ Mott insulator like the cuprates, but is chemically radically different[2,3]. Using spectroscopic-imaging STM, we find that for doping concentration of x≈5%, an inhomogeneous, phase separated state emerges, with the nucleation of pseudogap puddles around clusters of dopant atoms. Within these puddles, we observe the same glassy electronic order that is so iconic for the underdoped cuprates[1,4–9]. Further, we illuminate the genesis of this state using the unique possibility to localize dopant atoms on topographs in these samples. At low doping, we find evidence for much deeper trapping of carriers compared to the cuprates. This leads to fully gapped spectra with the chemical potential at mid-gap, which abruptly collapse at a threshold of around 4%. Our results clarify the melting of the Mott state, and establish phase separation and electronic order as generic features of doped Mott insulators.

2 A core mystery of condensed matter physics is how the rigid arrangement of electrons in Mott insulators loosens when inserting electrons or holes, and how this leads to exotic states inside the Mott gap (Fig. 1). In the cuprate high-temperature superconductors, this process might be the cause of their poorly understood, remarkably complex behavior. Most prominent is the formation of a pseudogap and a variety of inhomogeneous electronic orders[1,4–9], sometimes

described as intertwined[10]. This phenomenology has often been assumed (but not verified) to be generic of melting spin-½ Mott physics and not just cuprate-specific. In this Letter we show that an inhomogeneous electronic phase separation as well as a local glassy, stripy charge order exist in a chemically completely different two-dimensional Mott insulator, revealing the universality of these emergent phenomena.

3 To this end, we create $(Sr_{1-x}La_x)_2IrO_4$ samples with a range of different Lanthanum doping concentrations, $0<x<6\%$ (SI, Section 1). This material can be seen as a quasi two-dimensional, electron-doped Mott insulator similar to the cuprates despite a very different chemical make-up. The $x=0$ parent material consists of alternating IrO_2 and SrO planes, such that oxygen octahedra form around each iridium atom. The five valence electrons in the outer Ir 5*d* shell are split by crystal field and strong spin-orbit coupling to form a filled $J_{eff,3/2}$ and a half filled $J_{eff,1/2}$ band. The moderate on-site repulsion U is then sufficient to open a Mott gap in the $J_{eff,1/2}$ band, making Sr_2IrO_4 an effective spin-½ Mott insulator (Fig. 1a,b)[3]. In contrast to the hole doping in the cuprates, which is often interstitial oxygen doping, La^{3+} substitutions on the Sr site provide electron-doping for the iridates (Fig. 1c,d). The resulting electronic structure is sometimes predicted to become high-temperature superconducting upon sufficient doping[11,12].

4 We obtain atomically flat, SrO terminated surfaces for our measurements by mechanical cleaving of the $(Sr_{1-x}La_x)_2IrO_4$ samples in UHV at ~20K. All spectroscopic-imaging STM data is taken below 8K. Figures 1c,d depict typical topographs for different doping concentrations; the SrO lattice is visible with lattice constant $a_0=3.9$Å and the white squares identify the positions of La dopant atoms in the same layer[13]. The ability to identify the dopant positions easily with atomic precision on the topographs (e.g. in contrast to the cuprates[14,15]) is key to this investigation, as it allows to precisely localize dopant atoms, even when samples show micrometer variations of the dopant concentration (see SI, Sections 2,3). For this study, we investigate surfaces with local doping concentrations of 2.1%, 2.2% (Fig. 1d), 2.3%, 3.7%, 4.8%, 5.0% (Fig. 1e), 5.2%, 5.5% (Fig. 3,4) in order to obtain a full overview of the doping evolution (Fig. 5).

5 We start our discussion with the very lightly doped samples that are deep in the Mott phase. A typical topograph of a sample with 2.2% dopant concentration is shown in Figure 1c. In all our measurements, this doping level yields a clear Mott gap, as shown in Figure 2a. The shape of the gap is reminiscent of STM spectra of cuprate parent materials[5–7,16]. We describe in the SI, Section 4, how the poor screening in lightly doped Mott insulators leads to an additional potential that decays inside the sample, commonly called tip-induced-band-bending[17,18], yielding an apparent energy gap larger than true Mott gap, $\Delta^{app}_{Mott}>>\Delta_{Mott}$, which makes the gap roughly consistent with optical measurements[19].

6 To investigate how the Mott state reacts when dopant atoms are inserted, we acquire atomic-scale *Mott maps*, i.e. the magnitude of the Mott gap as a function of location, $\Delta_{\mathrm{Mott}}(\mathbf{r})$, while measuring the dopant positions on the atomic scale. Each Mott map is extracted from a set of differential conductance spectra measured on a grid (r_x,r_y). Figure 2a shows the result on a 2.2% sample; the dopant atoms are marked by green dots. La dopants do not significantly change the Mott gap size in their close vicinity; instead, they induce or pin long wavelength arrangement of varying Mott gap. We interpret these nanoscale arrangements as the first of a series of orders that appear upon doping. The most surprising observation, however, is the total lack of in-gap states, despite the presence of dopants – a mystery to which we shall return towards the end of this Letter.

7 The pure Mott state described thus far is not sustained at doping levels above ~5%. At that point, we discover an abrupt transition to a strikingly inhomogeneous electronic structure: a phase separated Mott/pseudogap landscape[20–22]. Some regions still exhibit a pure Mott gap. In contrast to the very low doping samples, now the Fermi level is pinned closer to the bottom of the upper Hubbard band, (blue curve in Fig. 3a), as expected for a Mott insulator doped with free carriers (similar to electron doped bi-layer iridate[23] and opposite to hole doped cuprates[6]). Additionally, there are regions where we measure electronic states inside the Mott gap (red curve in Fig. 3a). Here, the spectra are remarkably similar to the pseudogap in the cuprates[4–6], with a gap value of around 90-300meV, in rough agreement with recent photoemission measurements that extracted the leading edge gap[24–26]. We will refer to these regions as 'pseudogap puddles'. They are not randomly distributed, but form around regions with clusters of dopant atoms. Importantly, we do not observe pseudogap puddles in low doped samples, even if a few dopants happen to be close together by chance; a certain threshold in the doping level is needed for the transition to occur.

8 In order to further analyze this phase separated landscape, it is necessary to establish the spatial distribution of the Mott/pseudogap character. To do so, we introduce a "*Mott parameter*" $M(\mathbf{r})$ by integrating the density-of states inside the putative Mott gap and normalize it by the integrated density-of-states outside the gap, $M(\mathbf{r})=\int_{-350meV}^{+50meV} LDOS(E)dE \,/\, \int_{+200meV}^{+500meV} LDOS(E)dE$ (Fig. 3c, inset). This parameter is large when there are states inside the gap, and small when the Mott gap is dominating. Plotting $M(\mathbf{r})$ as a function of the spatial coordinates reveals the nanoscale character of the phase separation, with pseudogap puddles within regions of pure Mott gap. The phase separation is well defined and sharp, in the sense that the transition from pure Mott area to a pseudogap puddle occurs within less than a nanometer (Fig. 3d). This allows us to define a threshold for Mott and pseudogap regions (black contour in Fig. 3c).

9 We then develop a fitting procedure that is able to fit spectra both in the Mott regions and in the pseudogap puddles, capturing their vastly differing properties (Fig. 3b). We start with a smooth polynomial background density of states, and multiply it with a phenomenological Mott gap Δ_{Mott} consisting of two slightly broadened gap edges, asymmetric around the chemical potential. Next, we allow for states inside the Mott gap that are gapped by introducing a phenomenological function based on photoemission results[24,23] and commonly used in the cuprates[7,27]. This part allows for the extraction of the pseudogap value Δ_{PG}. The resulting model is an excellent fit to all the spectra measured on the highly doped samples, as shown in the SI, Section 7.

10 Extracting the gaps Δ_{PG} and Δ_{Mott} for 10^5 spectra located in the pseudogap puddles in a 17nm field of view allows us calculate the correlations between the two gaps. If the magnetic correlations J in the t-J model are directly causing order that manifests the pseudogap, one could expect an *anti*-correlation between Δ_{PG} and Δ_{Mott}, as $J \sim t^2/U$. Intriguingly, within the puddles, our data show a clear *positive* correlation of 0.31, i.e. the larger the Mott gap, the larger the pseudogap (Fig. 3e, inset). This is evidence that pseudogap and Mott physics are intimately linked[1,28], but suggests that it is not simply the magnetic correlations that cause the pseudogap.

11 To further test if the cuprate phenomenology is universal to lightly doped Mott insulators, we search for ordered phases on our samples. In the cuprates, it has become very clear that a sizable set of (possibly intertwined) orders coexist, perhaps causing the pseudogap[1]. These include disordered stripy charge arrangements, sometimes referred to as glassy order or charge density waves[1,4–10]. Indeed, we find that the spatial distribution of the pseudogap value, when extracted with atomic precision, reveals a striking tendency for order. The Δ_{PG} gap maps exhibit glassy, locally unidirectional structures (Fig. 3e and 4a), reminiscent of lightly hole doped cuprates[4–8](see SI, section 6). Glassy charge order is also visible in the density of states right outside the pseudogap, e.g. at -210meV shown in Figure 4b,c. The arrangements consist of bond centered, unidirectional objects of length-scales of 2 to 4 Ir-Ir distances, clearly very disordered on a larger length-scale. These arrangements, like the pseudogap puddles, nucleate around the dopant atom positions (green circles).

12 Next, we want to elucidate how this inhomogeneous, charge ordered pseudogap state emerges from the fully gapped state at low doping, by using the unique availability of samples with densely spaced doping concentrations in the iridate family. We measure one or more spectroscopic imaging maps with $>10^6$ data-points at each doping concentration, and we analyze each using the methods described above. Figure 5 summarizes the results, illustrating the abrupt nature of the transition. Panel **a** shows the evolution of the averaged spectra in the regions with pseudogap (red) and in those without (blue), panels **b**-**g** show the phase

separation on the respective field of views as defined by the Mott parameter defined above.

13 At doping concentration below the transition threshold, none of the spectra exhibits any sort of impurity state. Nor is the chemical potential pinned to one of the edges of the Mott gap, as one would expect from a Mott insulator with free carriers from shallow dopant centers. Combined with the fact that the phenomenology of the electronic structure is surprisingly independent of the doping concentration below ~4%, this leads to the question: Where did all the dopant electrons go? We propose the scenario illustrated in Figure 5h. Tightly bound dopant electrons at the dopant locations lead to a putative dopant band (impurity band in semiconductor parlance) inside the gap which keeps the chemical potential around mid-gap. Because the extra electrons from the La^{3+} dopants reside in the upper Hubbard band in the IrO layer, they experience the strong Mott correlations. Consequently, the charging energy $E=e^2/C$ to remove or add electrons (or holes) to the [La^{3+} + e^-] bound state is large, and this energy splits the dopant band (Fig. 5h). The reason that the gap is still flat is because in our case the splitting is large enough to push the dopant bands outside the Mott gap. An equivalent way of describing this, going back to N.F. Mott, is that there is a Mott transition in the dopant band[29]. In the cuprates, similar microscopic processes have initially been proposed, but the Mott state is much more fragile: even weak doping of around 2% can destroy the logarithmic divergence in the resistance[30]. Below that, however, it behaves similar to a doped semiconductor, with an impurity band close to the energy of the valence band[30]. This is consistent with the later observation that the dopant centers are quite shallow[6]. Based on our results, we predict that LDA+U calculations[3,31] on the iridates will reveal the trapping of La dopant states to be much deeper than the equivalent states in the cuprates, and that more homogenous samples will reveal a very sharp impurity band metal-insulator transition.

14 Finally, we would like to go back to the comparison of the electron doped iridate material studied here to the cuprates. Detailed measurements on the cuprates, e.g. $Ca_{2-x}Na_xCuO_2Cl_2$ and $Bi_2Sr_2CaCu_2O_{8+\delta}$, revealed surprising universalities including the glassy charge order observed in the CuO layer. On first look, $(Sr_{1-x}La_x)_2IrO_4$ seems to be a very different beast: electron instead of hole doping, Ir instead of Cu, $5d^5$ instead of $3d^9$. However, our data clearly shows that the physics of electronic order and the pseudogap are not specific to the cuprates but generic to lightly doped Mott insulators, and we believe that the interplay between dopants and order seen here holds for the cuprates as well. By extension, we can expect $(Sr_{1-x}La_x)_2IrO_4$ to become a high-temperature superconductor with only slightly higher doping concentration.

— — —

Acknowledgements: We thank J. Aarts, J.C. Davis, M.H. Hamidian, T. van Klingeren, Jhinhwan Lee, M. Leeuwenhoek, F.M. Massee, K. van Oosten, J. van Ruitenbeek, S. Tewari, G. Verdoes and J.J.T. Wagenaar for valuable discussions. We acknowledge funding from the *Netherlands Organization for Scientific Research* (NOW/OCW) as part of the *Frontiers of Nanofront program* and the *Vidi talent scheme*, and from the *Swiss National Science Foundation* (200021-146995).

Author contributions: I.B., K.B., V.F., M.P.A performed SI-STM experiments and analyzed data, C.H., A.T., R.P. created and characterized the samples, M.P.A. supervised the study. All authors contributed to the interpretation of the data.

References:

1. Keimer, B., Kivelson, S. A., Norman, M. R., Uchida, S. & Zaanen, J. From quantum matter to high-temperature superconductivity in copper oxides. *Nature* **518,** 179–86 (2015).

2. Rau, J. G., Lee, E. K.-H. & Kee, H.-Y. Spin-Orbit Physics Giving Rise to Novel Phases in Correlated Systems: Iridates and Related Materials. *Annu. Rev. Condens. Matter Phys.* **7,** 2.1–2.27 (2016).

3. Kim, B. J. *et al.* Novel j_{eff}=1/2 mott state induced by relativistic spin-orbit coupling in Sr2IrO4. *Phys. Rev. Lett.* **101,** 1–4 (2008).

4. Fujita, K. *et al. Spectroscopic Imaging STM: Atomic-Scale Visualization of Electronic Structure and Symmetry in Underdoped Cuprates. Theor. Methods Strongly Correl. Syst.* **Chapter 3,** (Springer Berlin Heidelberg, 2012).

5. Kohsaka, Y. *et al.* Imaging nanoscale electronic inhomogeneity in the lightly doped mott insulator $Ca_{2-x}Na_xCuO_2Cl_2$. *Phys. Rev. Lett.* **93,** 7–10 (2004).

6. Cai, P. *et al.* Visualizing the evolution from the Mott insulator to a charge ordered insulator in lightly doped cuprates. *ArXiv e-prints* (2015).

7. Kohsaka, Y. *et al.* Visualization of the emergence of the pseudogap state and the evolution to superconductivity in a lightly hole-doped Mott insulator. *Nat. Phys.* **8,** 534–538 (2012).

8. Parker, C. V *et al.* Fluctuating stripes at the onset of the pseudogap in the high-T(c) superconductor $Bi_2Sr_2CaCu_2O_{8+x}$. *Nature* **468,** 677–680 (2010).

9. Comin, R. & Damascelli, A. Resonant X-Ray Scattering Studies of Charge Order in Cuprates. *Annu. Rev. Condens. Matter Phys.* **7,** 369–405 (2016).

10. Fradkin, E., Kivelson, S. A. & Tranquada, J. M. Colloquium: Theory of intertwined orders in high temperature superconductors. *Rev. Mod. Phys.* **87,** 457–482 (2015).

11. Wang, F. A. & Senthil, T. Twisted hubbard model for Sr_2IrO4: Magnetism and possible high temperature superconductivity. *Phys. Rev. Lett.* **106,** 2–5 (2011).

12. Watanabe, H., Shirakawa, T. & Yunoki, S. Monte Carlo Study of an Unconventional Superconducting Phase in Iridium Oxide J_{eff}=1/2 Mott Insulators Induced by Carrier Doping. *Phys. Rev. Lett.* **110,** 027002 (2013).

13. Okada, Y. *et al.* Imaging the evolution of metallic states in a correlated iridate. *Nat. Mater.* **12,** 707–13 (2013).

14. McElroy, K. *et al.* Atomic-Scale Sources and Mechanism of Nanoscale Electronic Disorder in $Bi_2Sr_2CaCu_2O_{8+delta}$. *Science* **309,** 1048–1052 (2005).

15. Zeljkovic, I. *et al.* Imaging the Impact of Single Oxygen Atoms on Superconducting $Bi_{2+y}Sr_{2-y}CaCu_2O_{8+x}$. *Science (80-.).* **337,** 320–323 (2012).

16. Ye, C. *et al.* Visualizing the atomic-scale electronic structure of the $Ca_2CuO_2Cl_2$ Mott insulator. *Nat. Commun.* **4,** 1365 (2013).

17. Feenstra, R. M., Dong, Y., Semtsiv, M. P. & Masselink, W. T. Influence of tip-induced band bending on tunnelling spectra of semiconductor surfaces. *Nanotechnology* **18,** 044015 (2007).

18. Wijnheijmer, A. P. *et al.* Single Si dopants in GaAs studied by scanning tunneling microscopy and spectroscopy. *Phys. Rev. B* **84,** 125310 (2011).

19. Moon, S. J. *et al.* Temperature dependence of the electronic structure of the Jeff 1/2 Mott insulator. *Phys. Rev. B* **80,** 195110 (2009).

20. Chen, X. *et al.* Influence of electron doping on the ground state of $(Sr_{1-x}La_x)2IrO_4$. *Phys. Rev. B* **92,** 075125 (2015).

21. Yan, Y. J. *et al.* Electron-Doped Sr_2IrO_4: An Analogue of Hole-Doped Cuprate Superconductors Demo. *Phys. Rev. X* **5,** 041018 (2015).

22. Dai, J., Calleja, E., Cao, G. & McElroy, K. Local density of states study of a spin-orbit-coupling induced Mott insulator $Sr_2Ir\ O_4$. *Phys. Rev. B - Condens. Matter Mater. Phys.* **90,** 041102 (2014).

23. He, J. *et al.* Spectroscopic evidence for negative electronic compressibility in a quasi-three-dimensional spin-orbit correlated metal. *Nat. Mater.* **14,** 577–82 (2015).

24. Kim, Y. K. *et al.* Fermi arcs in a doped pseudospin-1/2 Heisenberg antiferromagnet. *Science* **345,** 187 (2014).

25. de la Torre, A. *et al.* Collapse of the Mott Gap and Emergence of a Nodal Liquid in Lightly Doped Sr_2IrO_4. *Phys. Rev. Lett.* **115,** 176402 (2015).

26. Kim, Y. K., Sung, N. H., Denlinger, J. D. & Kim, B. J. Observation of a d-wave gap in electron-doped Sr_2IrO_4. *Nat. Phys.* **12,** 1–6 (2015).

27. Alldredge, J. W. *et al.* Evolution of the electronic excitation spectrum with strongly diminishing hole density in superconducting $Bi_2Sr_2CaCu_2O_{8+\delta}$. *Nat. Phys.* **4,** 319–326 (2008).

28. Civelli, M., Capone, M., Kancharla, S. S., Parcollet, O. & Kotliar, G. Dynamical breakup of the fermi surface in a doped mott insulator. *Phys. Rev. Lett.* **95,** 2–5 (2005).

29. Mott, N. F. Metal-insulator transition. *Rev. Mod. Phys.* **40,** 677–683 (1968).

30. Kastner, M. A., Birgeneau, R. J., Shirane, G. & Endoh, Y. Magnetic, transport, and optical properties of monolayer copper oxides. *Rev. Mod. Phys.* **70,** 897–928 (1998).

31. Anisimov, V. I., Zaanen, J. & Andersen, O. K. Band theory and Mott insulators: Hubbard U instead of Stoner I. *Phys. Rev. B* **44,** 943–954 (1991).

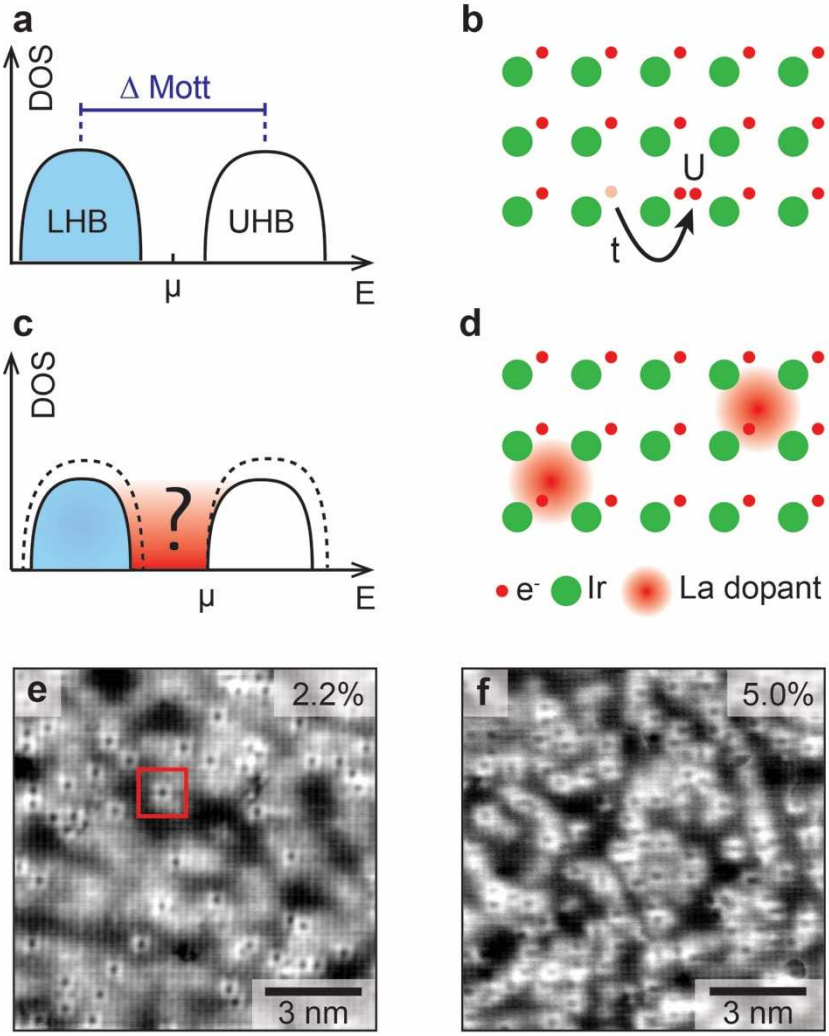

Figure 1. The lightly doped Mott insulator $(Sr_{1-x}La_x)_2IrO_4$. **a**, In Mott insulators, the electronic states split into a lower and upper Hubbard band separated by the Mott gap. **b**, The gap is caused by the on site interaction U that prevents electrons from hopping from site to site. **c**,**d,** When doping with charge carriers, new states move into the Mott gap in unknown ways. **e**, Atomically resolved topograph with a doping concentration 2.2% (see SI, Section 2). The La^{3+} dopant atoms are readily identified as dark spots surrounded by brighter atoms (red square)[12]. **d**, Atomically resolved topograph with a doping concentration of 5.0%. C.f. SI, Section 3 for more topographic images, and Section 4 for information on how we count the dopant atoms with precision of ±0.7%.

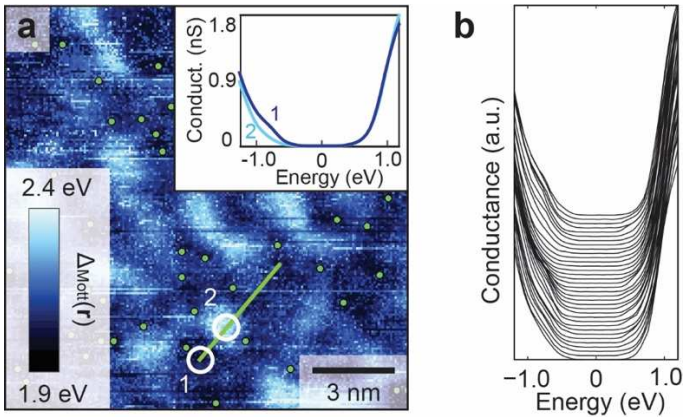

Figure 2. **a**, Mott gap map Δ_{Mott} of a sample with a doping concentration of x=2.2%. Position of dopant atoms are indicated by green circles. The inset shows local density of states spectra averaged inside the white circles. The additional density of states at around -0.8V is visible in the low gap regions, and might be related to the impending collapse of the impurity Mott state discussed later. **b**, Local density of states spectra along the green line in **a**, each with a relative shift on the vertical axis.

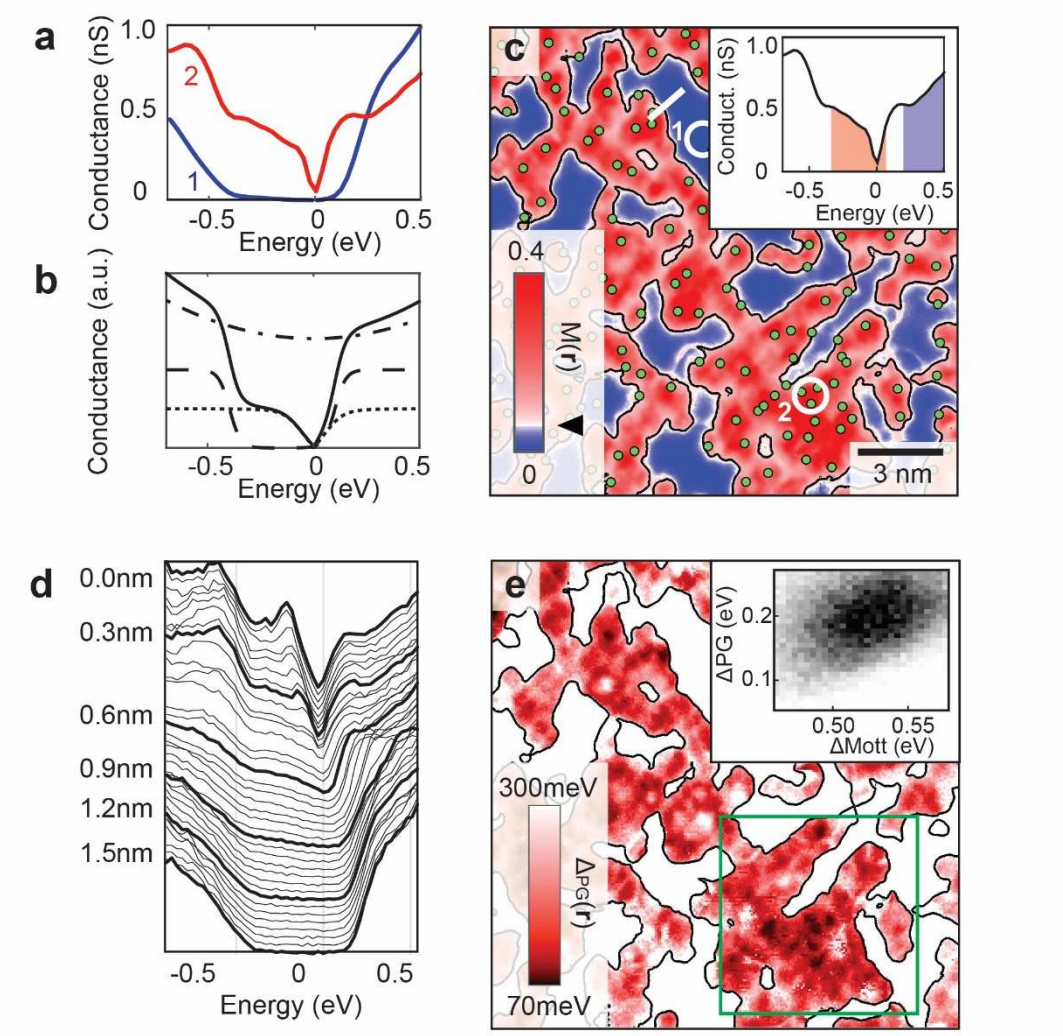

Figure 3. Phase separated Mott/pseudogap electronic structure at 5.5% doping. **a,** Different spectra in the phase separated region: Mott like spectrum (blue), with the chemical potential pinned to the UHB, and mixed Mott/pseudogap spectrum (red). The spectra are the average of 180 spectra inside the white circles in panel c. **b,** Phenomenological fit function to simultaneously extract both the Mott and pseudogap size. It consists of a density of states (dot-dashed) multiplied with Mott gap (dashed) plus states inside the Mott gap with a v-shaped pseudogap (dotted). See SI, Section 7 for details. **c,** The Mott parameter as defined in the text identifies pseudogap puddles (red) and pure Mott regions (blue). Green circles indicate La dopant locations. The triangle on the colorbar indicates the value of the black contour. Inset, definition of the Mott parameter: the integrated DOS inside Mott gap (red) normalized by the one outside the gap (blue). **d,** The separation is sharp in the sense that a Mott spectrum becomes a pseudogap spectrum within roughly a nanometer. **e**, Δ_{PG} map extracted from the fitting procedure (for Δ_{Mott}, see SI Section 6). The square indicates the region displayed in Figure 4. Inset**,** the correlation between Δ_{Mott} and Δ_{PG}.

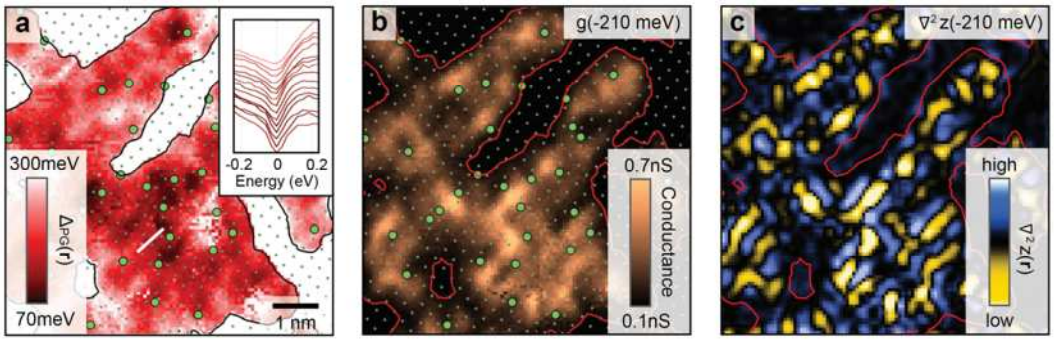

Figure 4. Nucleating order. **a**, Map of the pseudogap $\Delta_{PG.}$ The small green dots indicated Ir atom location, the larger green circles indicate La dopant locations on the Sr site. Disordered, locally unidirectional patterns are visible. The inset shows a series of spectra along the white line. The color indicates the gap value. **b**, Density of states at -210meV. Glassy order is nucleating around the La dopant atoms. **c**, Laplacian of the ratio map at -210meV.

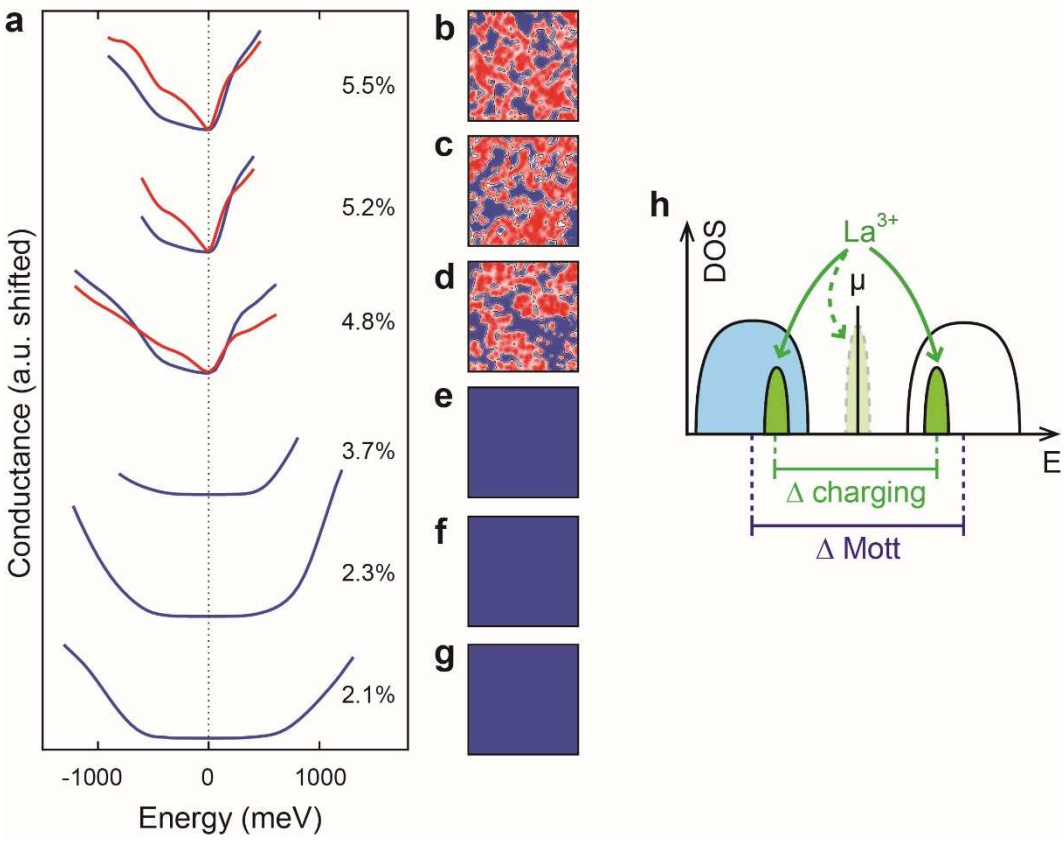

Figure 5. The evolution of the electronic structure with increasing dopant atom concentration. **a**, Differential conductance spectra at different doping levels, each averaged over regions with Mott gap (blue) and pseudogap (red) as defined by the Mott parameter in b-g. At around 5%, the phase separation abruptly starts. **b-g**, Respective maps of the Mott parameter, where blue indicates a pure Mott gap, and red indicates a pseudogap puddle. Increasing doping leads to smaller pure Mott areas. **h,** Schematic image of an impurity Mott transition, with the split impurity band states, (not) including the energy splitting $\Delta_{charging}$ in (light) green.